



CHORUS

This is the accepted manuscript made available via CHORUS. The article has been published as:

Origin of the positive spin-1/2 photoluminescence-detected magnetic resonance in π -conjugated materials and devices

Ying Chen, Min Cai, Emily Hellerich, Ruth Shinar, and Joseph Shinar

Phys. Rev. B **92**, 115203 — Published 2 September 2015

DOI: [10.1103/PhysRevB.92.115203](https://doi.org/10.1103/PhysRevB.92.115203)

**Origin of the Positive Spin 1/2 Photoluminescence-Detected Magnetic Resonance in
 π -Conjugated Materials and Devices**

Ying Chen,^{1*} Min Cai,¹ Emily Hellerich,¹ Ruth Shinar,² and Joseph Shinar^{1*}

¹*Ames Laboratory – USDOE and Physics & Astronomy Department*

²*Microelectronics Research Center and Electrical & Computer Engineering Department,*

Iowa State University, Ames, IA 50011

The spin-1/2 single modulation (SM) and double modulation (DM) photoluminescence (PL) detected magnetic resonance (PLDMR) in poly(2-methoxy-5-(2'-ethyl)-hexoxy-1,4-phenylene vinylene) (MEH-PPV) films and poly(3-hexylthiophene) (P3HT) films is described, analyzed, and discussed. In particular, the models based on spin-dependent recombination of charge pairs (SDR) and triplet-polaron quenching (TPQ) are evaluated. By analyzing the dependence of the resonance amplitude on the microwave chopping (modulation) frequency using rate equations, it is demonstrated that the TPQ model can well explain the observed resonance behavior, while SDR model cannot reproduce the results of the observed DM-PLDMR. Thus the observed spin-1/2 PLDMR is assigned to TPQ rather than SDR, even though the latter may also be present.

PACS Nos. 76.70.Hb, 82.35.Cd, 81.05.Fb

*Corresponding authors; emails chen2ying3@ufl.edu, jshinar@iastate.edu

Introduction

π -conjugated materials have attracted great interest due to their applications in organic light emitting diodes (OLEDs), solar cells, field effect transistors, and spintronic devices [1-4]. Spin-dependent phenomena in these organic semiconductors such as (i) triplet-by-polaron quenching (TPQ), i.e.,



where TE is a triplet exciton, $p^{+/-}$ is a positive or negative polaron, and $p^{+/-*}$ is an excited state of $p^{+/-}$, (ii) $p^+ + p^-$ recombination, and (iii) TE-TE annihilation play central roles in these applications. This is due to the fact that under typical steady-state photoexcitation or carrier-injection conditions, the population of polarons and TEs is $\sim 100\times$ and $\sim 10,000\times$, respectively, the population of singlet excitons (SEs).

Optically detected magnetic resonance (ODMR) is a powerful probe of the foregoing spin-dependent processes due to its high sensitivity [5]. In this technique, resonance conditions are achieved when the applied microwave photon energy matches the Zeeman splitting of spin sublevels, causing population mixing in these sublevels, and in turn leading to observable changes in optical properties, e.g., the photoluminescence (PL), photoinduced absorption (PA), or electroluminescence (EL). Moreover, electrically detected magnetic resonance (EDMR) in organic electronic devices has been demonstrated to enable robust absolute magnetometry with such devices [6]. By analyzing the behavior of the resonance, e.g. the magnetic resonance-induced change ΔI_{PL} , ΔI_{PA} , or ΔI_{EL} , respectively, under various conditions such as optical or electrical excitation power, microwave power, microwave modulation (chopping) frequency f_M , and temperature T , useful information such as the polaron lifetime τ_p and spin relaxation time T_2^* , which are crucial quantities for, e.g., organic

spintronics, can be obtained. Naturally, the correct interpretation of the resonance mechanism is essential to extract these values and provide valuable insight into the above-mentioned processes.

All the numerous studies reported to date described a positive (PL-enhancing) spin-1/2 PL-detected magnetic resonance (PLDMR) [5,7-13]. Yet two completely different mechanisms were proposed to explain the source of that resonance:

(i) Triplet-polaron quenching (TPQ). Here the PL is enhanced at resonance due to reduced quenching of the radiative SEs by TEs and polarons, as their populations are reduced at resonance due to the strongly spin-dependent TPQ process [5,9,10].

(ii) Spin-dependent recombination (SDR). Here the PL is enhanced due to an enhanced population of nongeminate singlet polaron pairs, which recombine to SEs, at the expense of triplet pairs, which would recombine to TEs [11-14].

Both processes have been observed in various organic semiconductor systems [15-21]. And both models can explain the enhancing nature of the spin 1/2 PLDMR. To determine which model should be used when analyzing the spin 1/2 PLDMR to extract useful information, the behavior of the resonance under various modulation conditions has been studied. In particular, the exciting laser modulation frequency $\omega_L = 2\pi f_L$ -dependence of the double modulation PLDMR (DM-PLDMR) of poly(2-methoxy-5-(2'-ethyl)-hexoxy-1,4-phenylene vinylene) (MEH-PPV) films is easily explained by TPQ, but impossible by SDR [9,10]. In DM-PLDMR, we use two lock-in amplifiers connected in series [9]: The first is referenced to the modulation frequency of the exciting laser power (" f_L lock-in"). *As such, it filters out the long-lived part of the PL, e.g., from SDR, that is too slow to follow the*

modulation of the laser power. Its output is fed to the input of the microwave modulation (chopping) frequency $\omega_M = 2\pi f_M$ -referenced lock-in (“ f_M lock-in”). But as the slower PL is filtered out by the f_L lock-in, the f_M lock-in only provides the PLDMR of the faster PL. Hence, if the PLDMR does not change as the laser power modulation frequency increases up to 100 kHz (= 1/(10 μ s)), that PLDMR cannot be coming from any delayed PL, particularly not from spin-dependent polaron recombination, most of which occurs on a longer time scale. Conversely, it was argued that TPQ cannot explain the phase change in the f_M -dependence of the single modulation PLDMR (SM-PLDMR) while SDR does [11,14]. Although a recent analytical study of the f_M -dependence of the SM-PLDMR showed that it is difficult to differentiate between different models by fitting the SM-PLDMR results [22], it did not provide details, particularly in fitting the resonance using the TPQ model. Thus, it is important to provide more results of spin $\frac{1}{2}$ SM- and DM-PLDMR in various systems and conditions and examine the ability of the models to fit *all* of the results, *both the SM- and DM-PLDMR.*

This paper describes the SM- and DM-PLDMR of poly(3-hexylthiophene) (P3HT) and MEH-PPV films and analyzes in detail the SM-PLDMR based on the TPQ model. *It shows that TPQ accounts for both PLDMRs, including the phase behavior, and should be the mechanism behind the positive spin $\frac{1}{2}$ PLDMR.*

Experimental Procedure

P3HT and MEH-PPV films were prepared by drop-casting films from toluene solutions onto the inner walls of quartz tubes that were then evacuated and sealed. The sample tube was

inserted into a quartz “finger dewar,” itself inserted in an X-band (~ 9.35 GHz) microwave cavity positioned between the poles of a dc magnet. The sample was excited at $\lambda = 488$ nm by an Ar^+ laser. The time constant of the f_L lock-in was set to 1 ms; f_M was constant at 200 Hz for DM-PLDMR, but was varied for SM-PLDMR.

Results, Analysis, and Discussion

In MEH-PPV films, the DM-PLDMR at $T = 20$ K does not decrease as f_L increases to 100 kHz [5,9,10]. *Hence this behavior demonstrates, independent of any model, that the resonance is not due to any contribution to the PL from processes slower than $\sim 1/10^5$ Hz = 10 μs .* This is due to the nature of the DM-PLDMR measurement, as the first lock-in amplifier filters out any signal that cannot follow the modulation of f_L . At high f_L , only “fast” PL ($\tau < 1/f_L$) can be detected. PL from slow processes such as delayed recombination of polarons would be filtered out by the first lock-in because it cannot be effectively modulated at this high frequency. As a consequence, the SDR model predicts a big decrease in the DM-PLDMR signal at f_L higher than polaron lifetime, because it suggests the PL responsible for the resonance signal comes solely from delayed polaron recombination. Yet it is well known that the polaron lifetimes are distributed widely and the majority’s lifetime is much longer than 10 μs [5, 23]. Hence at $f_L = 100$ kHz, according to SDR model, the DM-PLDMR signal should already be much smaller compared to the signal at low f_L . This prediction by SDR is obviously in contradiction with the observed DM-PLDMR behavior. On the other hand, as described in detail in Refs 9 and 10, TPQ explains this f_L dependence of the DM-PLDMR well. Unlike SDR, TPQ suggests that the resonance signal is due to the change

in the prompt fluorescence from SE recombination under resonance conditions. Under such conditions, the population of SEs increases due to reduced quenching, resulting in stronger prompt fluorescence. Because the majority of the PL comes from this *prompt* (~ 1 ns) fluorescence, the resonance signal is largely independent of polaron recombination. Even at the high $f_L \sim 100$ kHz, the signal from the prompt PL can still pass the first lock-in amplifier and the resonance signal should be largely unchanged.

It should be noted that pulsed EDMR measurements also demonstrate the presence of the TPQ process, at least at $T < 50$ K [21]. Hence it is more than plausible to assign the mechanism underlying the positive spin 1/2 PLDMR to TPQ. However, this spin 1/2 resonance is observable even at room temperature. Thus, the DM-PLDMR behavior at these temperatures should also be studied. Fig 1 shows the f_L dependence of this spin-1/2 DM-PLDMR at various temperatures. Even at room temperature, the intensity of the signal does not decrease with increasing f_L .

We further find that this behavior of the DM-PLDMR is not limited to MEH-PPV films. FIG. 2 shows the spin 1/2 DM-PLDMR of a P3HT film vs f_L . The inset shows the resonance line shape at $f_L = 100$ KHz. As seen, the amplitude of the resonance remains unchanged at all f_L . This is similar to the results for MEH-PPV films and again directly contradicts the SDR model [9,10]. This implies that *the mechanism responsible for the observed spin 1/2 PLDMR is TPQ, even though both the TPQ and SDR processes could exist simultaneously* [21].

It was argued that TPQ model has its own problem when it is used to explain the SM-PLDMR behavior [11, 14]. Figure 3 shows the f_M dependence of the SM-PLDMR in a MEH-PPV film at $T = 20$ K. The in-phase component X flips its sign at $f_M \approx 50$ kHz,

consistent with previous observations [11]. Indeed, using parameters from reference 10, one would not be able to reproduce the sign flipping. Although there is some phase shift, (here the phase is $\tan^{-1}(X/Y)$, where Y is the quadrature component), the in-phase signal X remains positive throughout the whole f_M range. It should be noted that those parameters used in reference 10 are related to actual physical quantities such as the TE population, polaron population, and TE-polaron interaction rate, and thus cannot be changed freely. Seemingly, therefore, the TPQ model fails to explain the observed sign-flipping behavior.

The foregoing calculations, however, are based on the approximation that the modulation is directly represented in the rate equations by the change in the quenching rate of TEs and polarons [10]. This is a good approximation when only the magnitude of the resonance is concerned, but requires re-examination to include phase information due to the additional phase lag of the TE-polaron recombination rate relative to the microwave modulation.

The mechanism wherein the TE-polaron quenching rate changes under resonance conditions can be explained as follows: Due to spin conservation, TPQ (Eq. (1)) occurs only in TE- $p^{+/-}$ pairs with spin 1/2 doublet (D) configuration; pairs in 3/2 quadruplet (Q) configuration will not undergo this process. Thus, combined with spin statistics, the off resonance D population will be lower than half of the off resonance Q population. On resonance, D and Q population mixing will increase the overall TPQ rate through the D recombination channel. This can be summarized in the rate equations

$$dQ/dt = G_Q - \frac{Q}{\tau_Q} - \frac{1}{T_{SL}}(Q - D) - (Q - D)P_{MW} \quad (2)$$

$$dD/dt = G_D - \frac{D}{\tau_D} + \frac{1}{T_{SL}}(Q - D) + (Q - D)P_{MW} \quad (3)$$

Here G_Q and G_D are the formation rates, τ_Q and τ_D are the lifetimes of the Q and D pairs, respectively, T_{SL} is the spin-lattice relaxation time of the colliding TE-polaron pairs, and P_{MW} is the μ wave-induced spin-flipping rate, which is proportional to the modulation depth. Due to their spin dependence, $\tau_Q > \tau_D$. Also, due to spin statistics, off-resonance the steady state population $Q_0 > D_0$.

Defining $Q(t)-Q_0 = \text{Re}\{Q^{0,1} e^{i\omega_M t}\}$ and similarly for $D^{0,1}$ and $P_{MW}^{0,1}$ leads to:

$$i\omega Q^{0,1} = -\frac{1}{\tau_Q} Q^{0,1} - \left(\frac{1}{T_{SL}} + P_0\right)(Q^{0,1} - D^{0,1}) - (Q_0 - D_0)P_{MW}^{0,1} \quad (4)$$

$$i\omega D^{0,1} = -\frac{1}{\tau_D} D^{0,1} + \left(\frac{1}{T_{SL}} + P_0\right)(Q^{0,1} - D^{0,1}) + (Q_0 - D_0)P_{MW}^{0,1} \quad (5)$$

Here P_0 is the average of the modulated P_{MW} . Solving Eqs. (4) and (5)-results in

$$\left[\frac{1}{4T_{SL-eff}^2 \left(i\omega + \frac{1}{\tau_Q} + \frac{1}{2T_{SL-eff}} \right)} + \left(i\omega + \frac{1}{\tau_D} + \frac{1}{2T_{SL-eff}} \right) \right] D^{0,1} = \left[1 - \frac{1}{2T_{SL-eff} \left(i\omega + \frac{1}{\tau_Q} + \frac{1}{2T_{SL-eff}} \right)} \right] (Q_0 - D_0)P_{MW}^{0,1} \quad (6)$$

and

$$Q^{0,1} = \frac{\left[\frac{1}{2T_{SL-eff}} D^{0,1} - (Q_0 - D_0)P_{MW}^{0,1} \right]}{\left(i\omega + \frac{1}{\tau_Q} + \frac{1}{2T_{SL-eff}} \right)} \quad (7)$$

where T_{SL-eff} is the effective relaxation time given by

$$\frac{1}{T_{SL-eff}} = \frac{1}{T_{SL}} + P_0. \quad (8)$$

The solutions for $Q^{0,1}$ and $D^{0,1}$ are

$$Q^{0,1} = (Q_x + Q_y i)(Q_0 - D_0)P_{MW}^{0,1} \quad (9)$$

$$D^{0,1} = (D_x + D_y i)(Q_0 - D_0)P_{MW}^{0,1} \quad (10)$$

Here Q_x , Q_y , D_x and D_y are real numbers obtained from Eqs. (6) and (7).

Since the change in the collision rate originates from the increase in D pairs, i.e., $D^{0,1}$, approximated to first order, the collision term in Ref. 10 is

$$\gamma TP = D / \tau_D \quad (11)$$

Where γ is the rate at which TEs are quenched by polarons. T and P are the TE and polaron populations, respectively. Off-resonance at steady state, $Q_0 - D_0$ should be proportional to $T_0 P_0$.

Under the same first order approximation,

$$\gamma^{0,1} = \text{const} \times (D_x + D_y i) / \tau_D \times P_{MW}^{0,1} \quad (12)$$

where $\gamma^{0,1}$ is defined in the same way as $D^{0,1}$ and $P_{MW}^{0,1}$. It can be viewed as the modulation depth of γ , and was approximated to represent the modulation itself in Ref. 10.

It can be seen that compared to the real modulation $P_{MW}^{0,1}$, $\gamma^{0,1}$ has an additional phase lag $\varphi = \tan^{-1}(D_y / D_x)$ which the approximation made in ref 10 neglected. Taking this effect into account, and modifying the $\gamma^{0,1}$ term in the calculations for SM-PLDMR in Ref 10 accordingly, the modified X and Y are

$$X = x \cos \varphi - y \sin \varphi \quad (13)$$

$$Y = x \sin \varphi + y \cos \varphi \quad (14)$$

where

$$x = \frac{z_m \cdot (p_{m1} \cdot p_{m2} - \omega^2) + \omega^2 \cdot (p_{m1} + p_{m2})}{(p_{m1} \cdot p_{m2} - \omega^2)^2 + (\omega \cdot (p_{m1} + p_{m2}))^2} \quad (15)$$

$$y = \frac{(p_{m1} \cdot p_{m2} - \omega^2 - z_m \cdot (p_{m1} + p_{m2})) \cdot \omega}{(p_{m1} \cdot p_{m2} - \omega^2)^2 + (\omega \cdot (p_{m1} + p_{m2}))^2} \quad (16)$$

are the original in-phase and quadrature components in Ref 10. Here $\omega = 2\pi \times f_M$, and z_m , p_{m1} and p_{m2} are zero and pole parameters, directly borrowed from Ref 10. The final simulated

f_M -dependence of X and Y within the TPQ model are shown in Figure 4. Experimental data are duplicated from Figure 3 for comparison. As seen, X flips its sign at a frequency f_0 ; the model yields $\tau_D = 500$ ns for $f_0 = 50$ kHz. Note this simulation is not a rigorous fitting for the experimental data due to the difficulty in fitting three different quantities in the same time. Yet it still agrees with the experimental results to a good extent. It should be pointed out that the magnitude of $\gamma^{0,1}$ also changes, becoming f_M -dependent (see Eq. (12)), while in ref 10 it was approximated to be f_M -independent. That change in the magnitude of $\gamma^{0,1}$, however, is relatively small throughout the experimental frequency range, indicating that the approximation in Ref 10 is adequate when only the magnitude is considered.

Another effect observed in SM-PLDMR is the microwave power dependence of f_0 [11]. This is immediately explained by Eq. (12), as the phase lag is a function of P_0 , i.e., the average of the modulated P_{MW} . The inset of Figure 4 shows the phase lag φ vs P_0 when $T_{SL} = 10$ μ s.

It should be noted that the structure of Equations 2 and 3 is similar to the rate equations in Ref. 11. One might think they would naturally produce similar results if the fitting parameters are the same. In fact, this is not correct. There are two key differences between the two situations: (i) The species involved in TPQ are polaron pairs and TEs, while in SDR they are just polaron pairs. The physical meaning of the parameters in the equations are totally different and could have very different values. (ii) More importantly, Unlike SDR which is a one-step process, TPQ is a two-step process. In the first step the modulation changes the recombination rate of T-P pairs, as in Equations 2 and 3. In the second step the population of polarons and TEs changes as the recombination rate changes and in turn leads to a change in

the SE population and the PL. The observed resonance is the final result of these two steps. Both steps contribute their own parts to the total phase shift and intensity change. Only some similarity in the mathematical treatment of SDR model and the first step of TPQ model does not guaranty any similarity in the final results. In fact, with the second step, the TPQ model gives quite different final expressions for the resonance signals from what the SDR model gives. It is because of this difference that the TPQ model can explain both the SM-PLDMR and DM-PLDMR behaviors while the SDR model has its difficulty in explaining the DM-PLDMR behavior.

Another question could be why the first step in this model is assigned to the TPQ process. To answer this question, the requirements for the processes involved in this two-step model must be clarified: For the first step, it must be a spin-dependent process due to the nature of magnetic resonance. However, the products of this process should not directly produce any change in luminescence, otherwise this would be the first order effect to be seen in ODMR and any indirect effects would be overwhelmed by it. Polaron pairs with opposite charge annihilating each other are thus excluded because in first order it would be exactly what SDR model predicted, i.e., spin-dependent recombination of polaron pairs to form singlets. Triplet-triplet annihilation should be excluded for the same reason because it also produce singlet excitons. Forming polaron pairs with the same charge (bipolarons) is another candidate. Actually, one negative spin-1/2 resonance in ODMR is assigned to bipolarons. However, it is different from the positive spin-1/2 resonance discussed here. In particular, in ELDMR both resonances can be seen at the same time [24], and hence should not be confused with each other. Thus, TPQ is the most likely process responsible for this step.

Summary & Concluding Remarks

In conclusion, the spin-1/2 DM-PLDMR of MEH-PPV films at different temperatures and that of P3HT films showed a behavior similar to previously reported DM-PLDMR results in MEH-PPV films at 20K. The observed behavior can only be explained by the TPQ mechanism. At the same time, a simulation of the spin-1/2 SM-PLDMR based on the TPQ mechanism is shown to reproduce *all* of the observed SM-PLDMR phenomena as well. In contrast, while the SDR model explains the SM-PLDMR very well, it is in stark contradiction with the DM-PLDMR results, rendering TPQ the only mechanism that accounts for all the PLDMR observations reported to date. *We note that this conclusion does not exclude the existence of SDR and in turn the possibility of higher SE yield. It only shows that the positive spin-1/2 PLDMR is a manifestation of TPQ rather than SDR*, rendering it an important tool to study the related device physics such as in degradation and efficiency roll-off.

Acknowledgements

Ames Laboratory is operated by Iowa State University for the US Department of Energy (USDOE) under Contract No. DE-AC 02-07CH11358. This work was supported by the Office of Basic Energy Science, Division of Materials Sciences and Engineering, USDOE.

REFERENCES

1. J. Shinar and R. Shinar, *J. Phys. D: Appl. Phys.* **41**, 133001 (2008).
2. G. Gelinck, P. Heremans, K. Nomoto, and T. D. Anthopoulos, *Adv. Mater.* **22**, 3778 (2010).
3. J. Clark and G. Lanzani, *Nat. Phot.* **4**, 438 (2010).
4. V. Dediu, M. Murgia, F. C. Matocota, C. Taliani, and S. Barbanera, *Solid State Commun.* **122**, 181 (2002).
5. J. Shinar, *Laser Phot. Rev.* **6**, 767 (2012).
6. W. J. Baker, K. Ambal, D. P. Waters, R. Baarda, H. Morishita, K. van Schooten, D. R. McCamey, J. M. Lupton, and C. Boehme, *Nat. Comm.* **3**, 898 (2012).
7. L. S. Swanson, J. Shinar, and K. Yoshino, *Phys. Rev. Lett.* **65**, 1140 (1990).
8. J. Shinar, in *Handbook of Organic Conductive Molecules and Polymers*, edited by H. S. Nalwa (Wiley, New York, 1997), p.319.
9. M.-K. Lee, M. Segal, Z. G. Soos, J. Shinar, and M. A. Baldo, *Phys. Rev. Lett.* **94**, 137403 (2005).
10. M. Segal, M. A. Baldo, M. K. Lee, J. Shinar, and Z. G. Soos, *Phys. Rev. B* **71**, 245201 (2005).
11. C. G. Yang, E. Ehrenfreund, and Z. V. Vardeny, *Phys. Rev. Lett.* **99**, 157401 (2007).
12. M. Wohlgenannt, X. M. Jiang, Z. V. Vardeny, and R. A. J. Janssen, *Phys. Rev. Lett.* **88**, 197401 (2002)
13. M. Wohlgenannt, Kunj Tandon, S. Mazumdar, S. Ramasesha, and Z. V. Vardeny, *Nature* **409**, 494 (2001)

14. C. G. Yang, E. Ehrenfreund, M. Wohlgenannt, and Z. V. Vardeny, *Phys. Rev. B* **75**, 246201 (2007).
15. Y. Cao, I. D. Parker, G. Yu, C. Zhang, and A. J. Heeger, *Nature* **397**, 414 (1999).
16. P. K. H. Ho, J. S. Kim, J. H. Burroughes, H. Becker, S. F. Y. Li, T. M. Brown, F. Cacialli, and R. H. Friend, *Nature* **404**, 481 (2000).
17. D. Beljonne, A. Ye, Z. Shuai, and J. L. Brédas, *Adv. Funct. Mater.* **14**, 684 (2004).
18. A. S. Dhoot, D. S. Ginger, D. Beljonne, Z. Shuai, and N. C. Greenham, *Chem. Phys. Lett.* **360**, 195 (2002).
19. D. Hertel and K. Meerholz, *J. Phys. Chem. B* **111**, 12075 (2007).
20. Y. Meng, X. J. Liu, B. Di and Z. An, *J. Chem. Phys.* **131**, 244502 (2009)
21. W. J. Baker, D. R. McCamey, K. J. van Schooten, J. M. Lupton, C. Boehme, *Phys. Rev. B* **84**, 165205 (2011)
22. S. Y. Lee, S. Paik, D. R. McCamey and C. Boehme, *Phys. Rev. B* **86**, 115204 (2012).
23. *Semiconductor and Metal nano-crystals: Synthesis and Electronic and Optical Properties*, page 254, Edited by V. I. Klimov, CRC press, 2003
24. G. Li, C. H. Kim, P. A. Lane and J. Shinar, *Phys. Rev. B* **69**, 165311 (2004).

FIGURE CAPTIONS

FIG 1. DM-PLDMR vs f_L in MEH-PPV film at various temperatures:

(a) $T = 300\text{K}$, (b) $T = 160\text{K}$, (c) $T = 100\text{K}$ and (d) $T = 50\text{K}$. μ -wave power $P_M = 810\text{mW}$, laser power $P_L = 10 \text{ mW/mm}^2$.

FIG 2. Spin 1/2 DM-PLDMR signal intensity in a P3HT film vs. f_L at $T = 20\text{K}$; $f_M = 200 \text{ Hz}$.

Dashed line: Spin 1/2 DM-PLDMR vs. f_L predicted by the SDR model [9,10]. Inset: The line shape of the spin 1/2 DM-PLDMR at $f_L = 100 \text{ KHz}$.

FIG 3. The measured f_M dependence of the in-phase component X , the quadrature component Y , and modulus R (all absolute values) of the SM-PLDMR in MEH-PPV films. Note that the drop in X around $f_M = f_0$ is due to a change in the sign of X .

FIG 4. Simulated PLDMR under the TPQ model, which takes the phase shift in γ into account. $R(\text{sim})$, $X(\text{sim})$ and $Y(\text{sim})$ are the simulated PLDMR signals. R , X and Y are experimental data replicated from Figure 3 to be compared with the simulated result. Inset: The phase lag ϕ vs microwave power P_0 when $T_{SL} = 10 \mu\text{s}$.

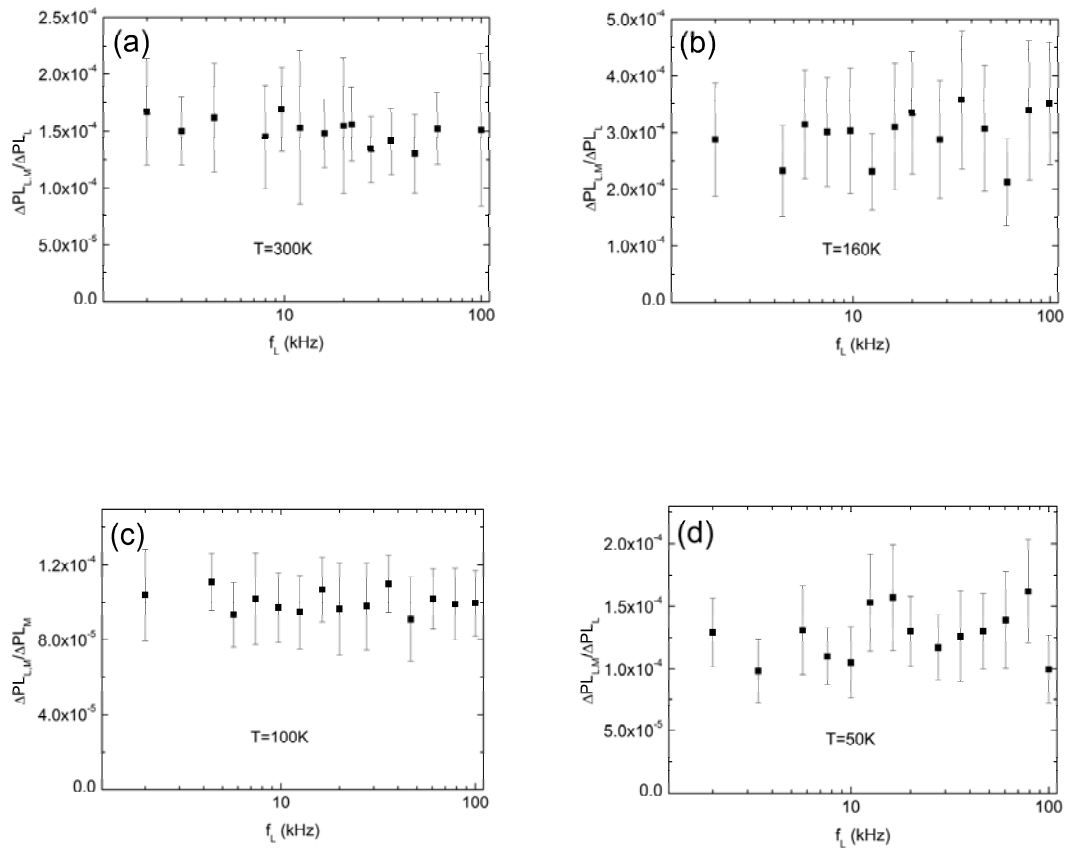


FIG 1. DM-PLDMR vs f_L in MEH-PPV film at various temperatures:

(a) $T = 300\text{K}$, (b) $T = 160\text{K}$, (c) $T = 100\text{K}$ and (d) $T = 50\text{K}$. μ -wave power $P_M = 810\text{mW}$, laser power $P_L = 10 \text{ mW/mm}^2$.

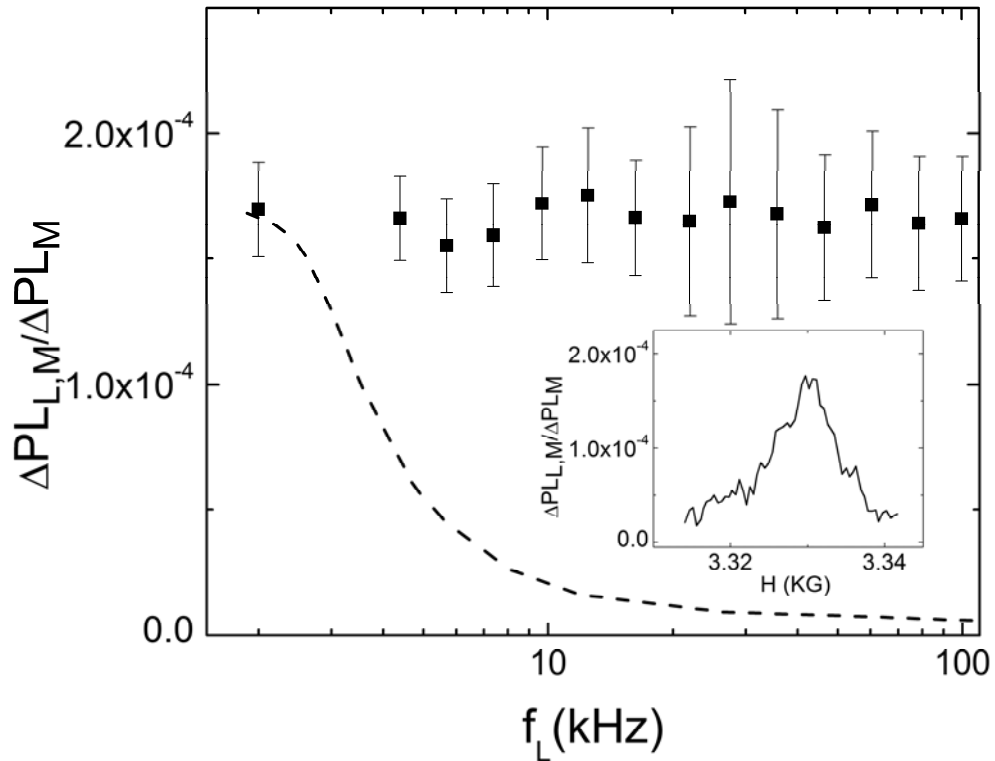


FIG. 2. Spin 1/2 DM-PLDMR signal intensity in a P3HT film vs. f_L at $T = 20\text{K}$; $f_M = 200$ Hz. Dashed line: Spin 1/2 DM-PLDMR vs. f_L predicted by the SDR model [9,10]. Inset: The line shape of the spin 1/2 DM-PLDMR at $f_L = 100$ KHz.

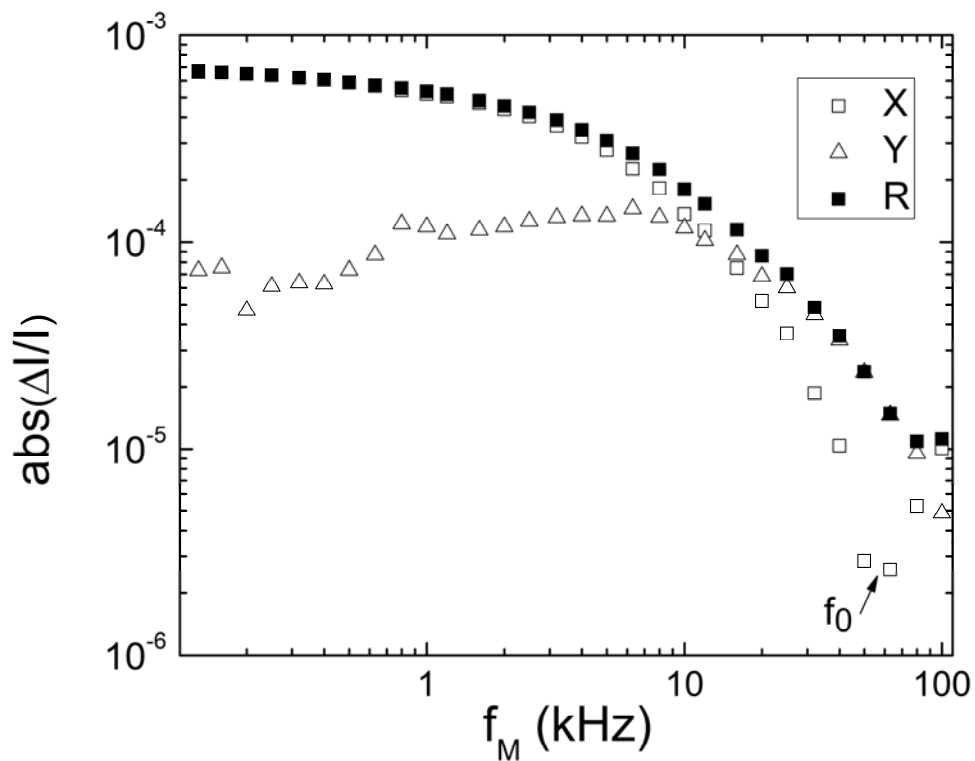


FIG. 3. The measured f_M dependence of the in-phase component X , the quadrature component Y , and modulus R (all absolute values) of the SM-PLDMR in MEH-PPV films. Note that the drop in X around $f_M = f_0$ is due to a change in the sign of X .

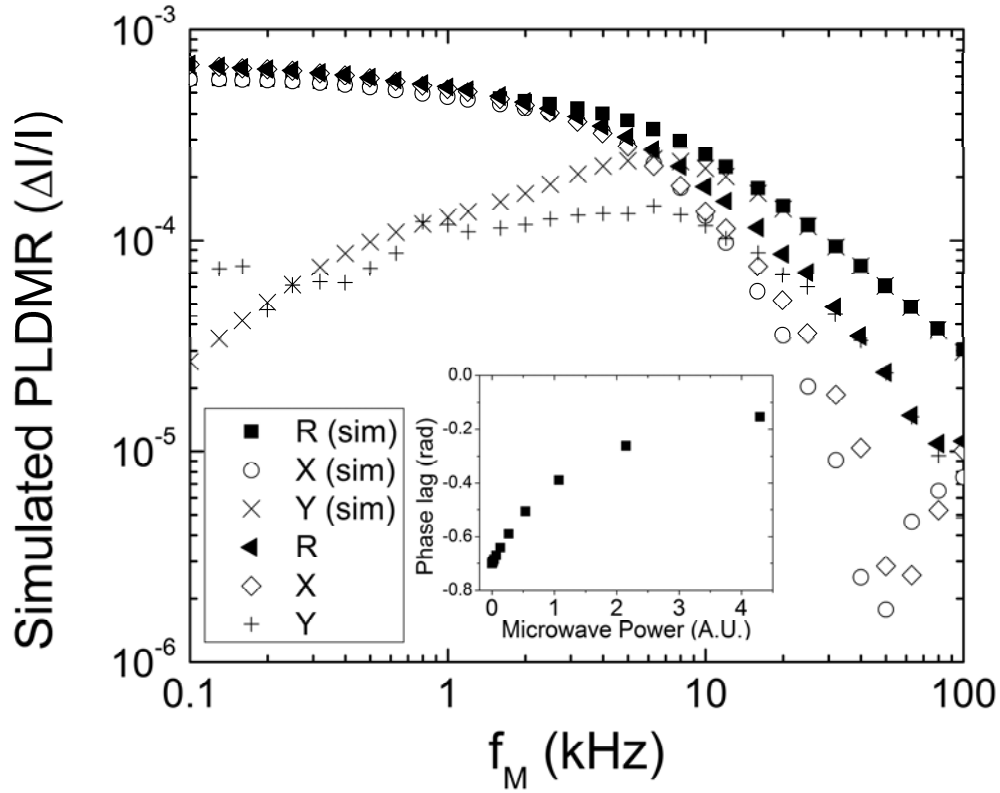


FIG. 4. Simulated PLDMR under the TPQ model, which takes the phase shift in γ into account. R(sim), X(sim) and Y(sim) are the simulated PLDMR signals. R, X and Y are experimental data replicated from Figure 3 to be compared with the simulated result. Inset: The phase lag φ vs microwave power P_0 when $T_{SL} = 10 \mu\text{s}$.